Gas-Phase Reaction of Tetraborane(10) and Ethyne: Molecular Structure of *nido*-1,2-$C_2B_3H_7$ in the Gas Phase

Mark A. Fox, Robert Greatrex,* and Alireza Nikrahi

School of Chemistry, University of Leeds, Leeds, LS2 9JT, U.K.

Paul T. Brain, Matthew J. Picton, David W. H. Rankin,* and Heather E. Robertson

Department of Chemistry, University of Edinburgh, West Mains Road, Edinburgh, EH9 3JJ, U.K.

Michael Bühl

Institüt fur Organische Chemische, Universität der Zürich, Winterthurerstrasse 190, CH-8057, Zürich, Switzerland

Linda Li and Robert A. Beaudet

Department of Chemistry, University of Southern California, University Park, Los Angeles, California 90089-0482

Received November 6, 1997

The molecular structure of *nido*-1,2-$C_2B_3H_7$, **1**, the principal volatile carborane generated in the quenched gas-phase reaction of B_4H_{10} and ethyne at 70 °C, has been determined by a combined analysis of gas-phase electron-diffraction data and rotation constants restrained by *ab initio* computations at the CCSD(T)/TZP′ level. The structure is consistent with a geometry having C_s symmetry, similar to that of pentaborane(9). The apical position is occupied by a carbon atom, displaced toward B(4) from a position directly above the B(5)···B(3) vector, and hydrogen atoms asymmetrically bridge the B−B bonds. The basal atoms are almost coplanar, C(2) lying *ca*. 2° below the B(3)−B(4)−B(5) plane. Important experimental structural parameters (r_α°/pm, $\angle_\alpha$/°) are r[C(1)−C(2)] = 162.6(6); r[C(1)−B(3)] = 161.4(3); r[C(2)−B(3)] = 154.3(2); r[C(1)−B(4)] = 157.4(5); r[B(3)−B(4)] = 185.7(3); <B(3)−B(4)−B(5) = 80.9(1). In addition to this and the other previously reported carboranes, 2,3-$C_2B_4H_8$, 2-Me-2,3,4-$C_3B_3H_6$, and 4-Me-2-CB_5H_8, several new derivatives have been identified among the volatile products. These include the dicarbahexaboranes 2,4-Me_2-2,3-$C_2B_4H_6$ and 5-Et-2,3-$C_2B_4H_7$ (the major volatile products obtained when the reaction is allowed to go to completion, previously reported as tricarbahexaboranes) and the derivatives 2,5-Me_2-2,3-$C_2B_4H_6$, 4-Et-2,3-$C_2B_4H_7$, 1-Me-2,3,4-$C_3B_3H_6$, 2-Me-2-CB_5H_8, 3-Me-2-CB_5H_8, and 2,3,4,5-$C_4B_2H_6$. The complex mechanism of the reaction is discussed in light of these new results.

Introduction

In a series of papers published between 1966 and 1972, Grimes and co-workers reported the results of investigations into the complex gas-phase reactions between tetraborane(10) and various alkynes at temperatures in the range 25−70 °C.[1−8] The reaction between B_4H_{10} and ethyne at 25−50 °C was reported to yield many volatile *nido*-carboranes, including 1,2-$C_2B_3H_7$ (**1**), 2,3-$C_2B_4H_8$ (**2a**), 2-Me-2,3,4-$C_3B_3H_6$ (**3a**), 2,3-Me_2-2,3,4-$C_3B_3H_5$ (**3b**), 2,4-Me_2-2,3,4-$C_3B_3H_5$ (**3c**), and 4-Me-2-CB_5H_8 (**4a**) (see Figure 1).

The parent *nido*-dicarbapentaborane **1** was found to be the major product when the B_4H_{10}/ethyne reaction at 50 °C was quenched[5−7] but was not observed when the reaction was allowed to proceed to completion. The product was stable in the gaseous state at 50 °C but decomposed in the liquid state to give a white solid. It also decomposed rapidly in the presence of B_4H_{10} to give 2-$MeCB_5H_8$ (**4b**), and reacted slowly with ethyne to yield $C_4B_2H_6$ (**5**); solids were produced in each case.[7,8] The yields of the derivatives reported at the time as the tricarboranes **3a**−**c** were unaltered when the B_4H_{10}/ethyne reaction was carried out in the presence of **1**.

The preliminary results of a microwave (MW) study of 1,2-$C_2B_3H_7$ (**1**) have been reported by Beaudet,[9] but the geometric

* Corresponding authors.

(1) Bramlett, C. L.; Grimes, R. N. *J. Am. Chem. Soc.* **1966**, *88*, 4269.
(2) Grimes, R. N.; Bramlett, C. L. *J. Am. Chem. Soc.* **1967**, *89*, 2557.
(3) Grimes, R. N.; Bramlett. C. L.; Vance, R. L. *Inorg. Chem.* **1968**, *7*, 1066.
(4) Franz, D. A.; Howard, J. W.; Grimes, R. N. *J. Am. Chem. Soc.* **1969**, *91*, 4010.
(5) Franz, D. A.; Grimes, R. N. *J. Am. Chem. Soc.* **1970**, *92*, 1438.
(6) Franz, D. A.; Grimes, R. N. *J. Am. Chem. Soc.* **1971**, *93*, 387.
(7) Franz, D. A.; Miller, V. R.; Grimes, R. N. *J. Am. Chem. Soc.* **1972**, *94*, 412.
(8) Miller, V. R.; Grimes, R. N. *Inorg. Chem.* **1972**, *11*, 862.
(9) Beaudet, R. A. In *Advances in Boron and the Boranes*; Liebman, J. F., Greenberg, A., Williams, R. E., Eds.; VCH Publishers: New York, 1988; Chapter 20.

S0020-1669(97)01395-5 CCC: $15.00
Published on Web 04/15/1998

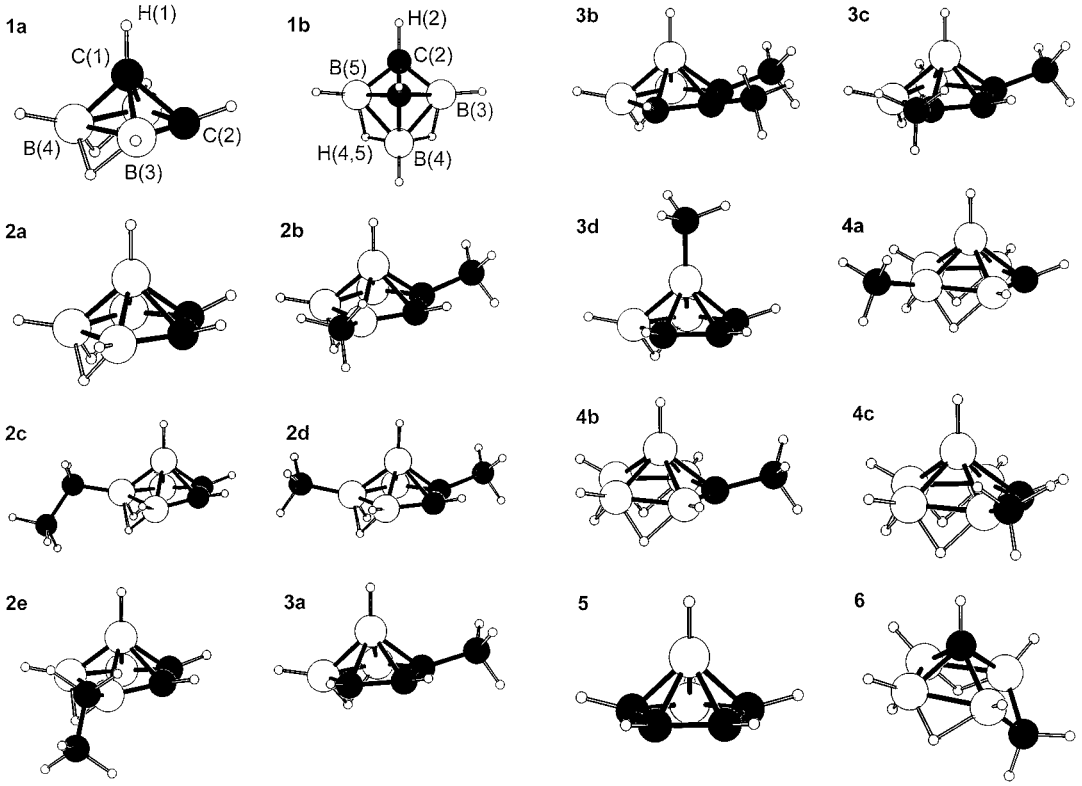

Figure 1. Range of volatile products from the reaction of B_4H_{10} and HC≡CH, including views of 1,2-$C_2B_3H_7$ in the optimum refinement of the electron-diffraction data; (a) perspective view and (b) perpendicular to the molecular C_s plane.

parameters show large, significant differences from those obtained by *ab initio* optimizations.[10] Comparison of the newly measured experimental ^{11}B NMR chemical shifts[11] with values calculated by the IGLO[10] and GIAO[11,12] NMR methods supports the structure derived from *ab initio* optimizations but not from the microwave study.

When dideuterioethyne was used instead of ethyne in the reaction with B_4H_{10}, all deuterium atoms in the products were found to be bound to carbon atoms.[4−6] The deuterated analogues of the derivatives **3a**−**c** were shown by mass spectrometry to contain three or four deuterium atoms, the relative abundance of tetra *vs* trideuterated derivatives increasing approximately 4-fold when the DC≡CD/B_4H_{10} ratio was changed from 1:1 to 10:1. The presence of B_2H_5D suggested that exchange of deuterium occurred between the carboranes and B_2H_6.

On the basis of a kinetic study of the B_4H_{10}/HC≡CH reaction, Franz and Grimes suggested that the rate-determining step involved the elimination of dihydrogen from B_4H_{10} to give the nonisolable intermediate $\{B_4H_8\}$.[6] The involatile solids were thought to arise from the successive addition of molecular ethyne to $\{B_4H_8\}$, and the formation of the various volatile products was explained in terms of slower side reactions involving nonisolable carborane intermediates (Scheme 1).

In a recent communication, Fox and Greatrex showed that two products from the B_4H_{10}/HC≡CH reaction reported previously as tricarbahexaboranes, *viz.* 2,3-$Me_2C_3B_3H_5$ (**3b**) and 2,4-Me_2-2,3,4-$C_3B_3H_5$ (**3c**), are in fact the dicarbahexaboranes 2,4-Me_2-2,3-$C_2B_4H_6$ (**2b**) and 5-Et-2,3-$C_2B_4H_7$ (**2c**), respectively.[13]

Scheme 1

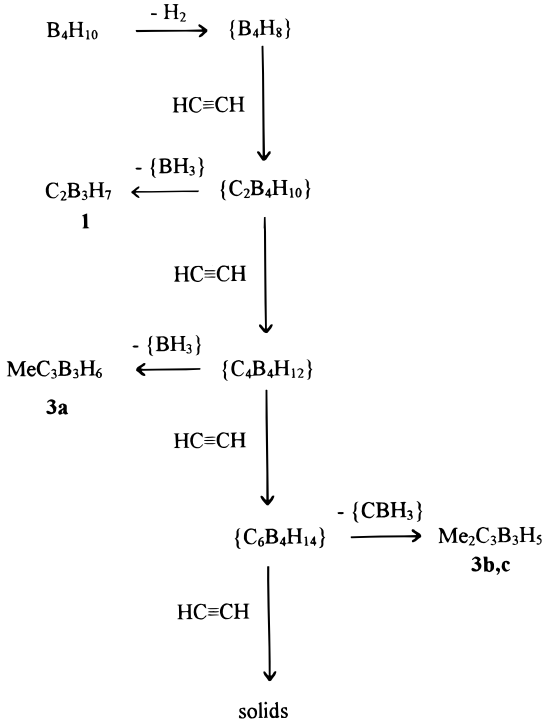

Incorporating these results into his computational study, McKee has suggested that the reactive intermediate $\{B_3H_7\}$ might be as important as $\{B_4H_8\}$ in accounting for the various products.[14,15] His proposed mechanism, which is summarized in

(10) Bühl, M.; Schleyer, P. v. R. *J. Am. Chem. Soc.* **1992**, *114*, 477.
(11) Schleyer, P. v. R.; Gauss, J.; Bühl, M.; Greatrex, R.; Fox, M. A. *J. Chem. Soc., Chem. Commun.* **1993**, 1766.
(12) Bühl, M.; Gauss, J.; Hofmann, M.; Schleyer, P. v. R. *J. Am. Chem. Soc.* **1993**, *115*, 12385.
(13) Fox, M. A.; Greatrex, R. *J. Chem. Soc., Chem. Commun.* **1995**, 667.
(14) McKee, M. L. *J. Am. Chem. Soc.* **1995**, *117*, 8001.
(15) McKee, M. L. *J. Am. Chem. Soc.*, **1996**, *118*, 421.

Scheme 2

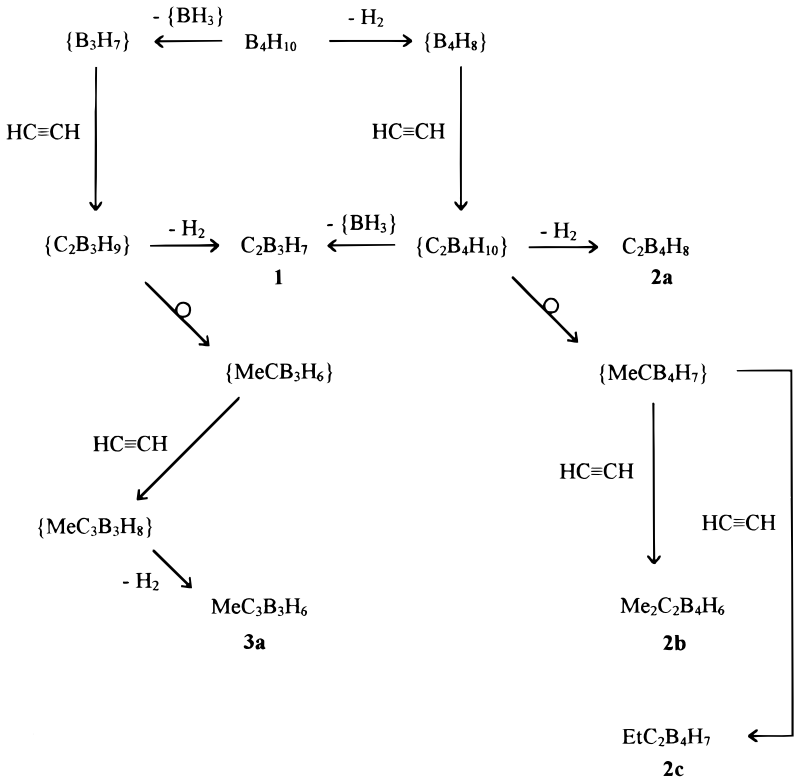

Scheme 2, involves two concurrent initial modes of decomposition to generate the reactive intermediates: loss of H_2 and loss of $\{BH_3\}$.

In this paper, as part of a continuing study of gas-phase reactions of B_4H_{10} with unsaturated hydrocarbons,[13,16−20] we report more fully the results of a reinvestigation of the products of the quenched and of the completed reactions of B_4H_{10} and HC≡CH at 70 °C and discuss the mechanistic implications. In addition, the molecular structure of *nido*-1,2-$C_2B_3H_7$ (**1**), the unstable main product of the quenched reaction, has been determined in the gas phase by a combined analysis of electron-diffraction (GED) data and rotation constants restrained by *ab initio* computations.

Experimental Section

General. All reactions were carried out in standard high-vacuum systems fitted wth greaseless O-ring taps and spherical joints (J. Young [Scientific Glassware] Ltd.). Mass spectrometric techniques developed in our earlier studies of binary borane interconversion reactions[21] were used to monitor the gas-phase reactions and to determine the optimum stage at which to quench the products, but no attempt was made to develop a rigorous quantitative analytical technique for the analytically more complex carborane system. The 1-liter Pyrex bulb used for the monitored reactions was enclosed in an isothermal oven and attached *via* Veridia capillary tubing (180 mm, 0.1 mm internal diameter) to a Kratos MS30 mass spectrometer. The latter was controlled by an MSS data system (Mass Spectrometry Services Ltd.). The high-vacuum, low-temperature fractionating column, which was a modification of that described in the literature,[22] was similarly connected to the mass spectrometer so that the volatile products could be monitored as they were pumped into U-traps cooled to 77 K. Tetraborane(10) was produced from $NMe_4B_3H_8$ (Alfa Products) and BF_3 (Cambrian Gases) by reported methods.[23] Ethyne (BOC) was obtained commercially and used as supplied.

Samples for NMR spectroscopy were transferred *in vacuo* to resealable 5 mm Young's tubes. Low-field measurements were made at 2.35 tesla (100 MHz ^{1}H) on a JEOL FX100 instrument, and high-field spectra were obtained at 9.4 tesla (400 MHz ^{1}H; 128 MHz ^{11}B; 100 MHz ^{13}C) on a Bruker AM-400 instrument with $CDCl_3$ as lock solvent at 298 K unless otherwise stated. Subtracted ^{1}H{^{11}B selective} and line-narrowed 2D ^{11}B−^{11}B COSY experiments were carried out as described elsewhere.[24]

Continuous Monitoring of the 1:1 B_4H_{10}/HC≡CH Reaction at 70 °C. Ethyne (0.5 mmol) and an equimolar amount of tetraborane-(10) were measured manometrically and condensed in turn into a phial. The mixture was then warmed to room temperature and bled into the preheated (70 °C) reaction vessel. After a few seconds the vessel was sealed. From the measured gas pressure of 7.5 mmHg, it was estimated that 0.35 mmol of the mixture was enclosed in the vessel. The reaction was monitored mass spectrometrically until no significant change in the spectrum was observed. The concentrations of B_4H_{10} and 1,2-$C_2B_3H_7$ were indicated by the intensities of the peaks in the ranges *m*/*z* 45−52 and 58−64, respectively, and ethyne from the intensity of the peak at *m*/*z* 26. A typical schematic profile of the reaction is shown in Figure 2.

Quenched Reactions of B_4H_{10} and Ethyne. A 1:1 mixture of tetraborane(10) (0.5 mmol) and ethyne (1.0 mmol) was made up as

(16) Fox, M. A.; Greatrex, R.; Hofmann, M.; Schleyer, P. v. R. *Angew Chem.* **1994**, *106*, 2384; *Angew. Chem., Int. Ed. Engl.* **1994**, *33*, 2298.
(17) Hofmann, M.; Fox, M. A.; Greatrex, R.; Schleyer, P. v. R.; Bausch, J. W.; Williams, R. E. *Inorg. Chem.* **1996**, *35*, 6170.
(18) Fox, M. A.; Greatrex, R.; Nikrahi, A. *Chem. Commun.* **1996**, 175.
(19) Fox, M. A.; Greatrex, R.; Hofmann, M.; Schleyer, P. v. R.; Williams, R. E. *Angew. Chem.* **1997**, *36*, 1498.
(20) (a) Brain, P. T.; Bühl, M.; Fox, M. A.; Greatrex, R.; Leuschner, E.; Picton, M. J.; Rankin D. W. H.; Robertson, H. E. *Inorg. Chem.* **1995**, *34*, 2841. (b) Hynk, D.; Brain, P. T. Rankin, D. W. H.; Robertson, H. E.; Greatrex, R.; Greenwood, N. N.; Kirk, M.; Bühl, M.; Schleyer, P. v. R. *Inorg. Chem.* **1994**, *33*, 2572.
(21) Greatrex, R.; Greenwood, N. N.; Waterworth, S. D. *J. Chem. Soc., Dalton Trans.* **1991**, 643 and references therein.
(22) Dobson, J.; Schaeffer, R. *Inorg. Chem.* **1970**, *9*, 21.
(23) Toft, M. A.; Leach, J. B.; Himpsl, F. L.; Shore, S. G. *Inorg. Chem.* **1982**, *21*, 195.
(24) Bown, M.; Plesek, J.; Base, K.; Stibr, B.; Fontaine, X. L. R.; Greenwood, N. N.; Kennedy, J. D. *Magn. Reson. Chem.* **1989**, *27*, 947.

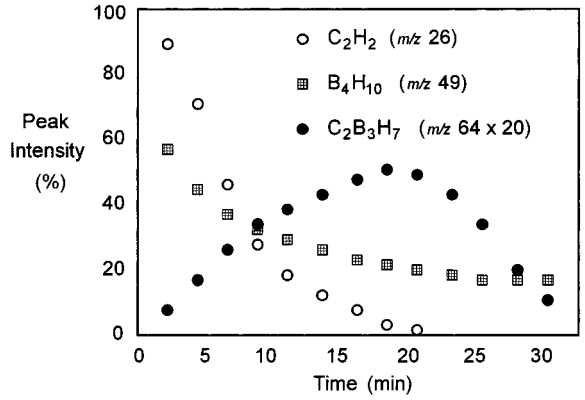

Figure 2. A typical profile of intensity (%) *vs* time (min) for selected peaks in the mass spectrum of the volatile products of the 1:1 B_4H_{10}/HC≡CH gas-phase reaction at 70 °C.

described above and expanded into the reaction bulb at 70 °C. The mixture (0.47 mmol; pressure = 10 mmHg) was monitored by mass spectrometry, and when the ethyne peak (*m*/*z* 26) had just disappeared (after *ca*. 45 min) the products were condensed into a U-trap. The amount of B_4H_{10} that could be used in the 1-L reaction vessel was limited to 0.5 mmol by the need to maintain an acceptable working pressure in the mass spectrometer. In order to accumulate sufficient product for the electron-diffraction study of 1,2-$C_2B_3H_7$ (*ca.* 0.3 g; 5 mmol) the process was repeated numerous times. The combined volatile products were then subjected to a cold-column fractionation, and the resulting fractions, characterized by different mass cutoffs, were studied by high-field ^{11}B and ^{1}H NMR spectroscopy (*J* values below in Hz).

1,2-$C_2B_3H_7$[5−7] (1). Approximate yield, 25% of boron used: 90% of total volatile carborane fraction; $\delta(^{11}B)$ at 233 K −13.4 (dd, 2B, J_{BHt} = 174, $J_{BH\mu}$ = 42; B3,5), −15.1 (dt, 1B, J_{BHt} = 174, $J_{BH\mu}$ = 50; B4); $\delta(^{13}C)$[11] 57.9, C2; −21.5, C1; $\delta(^1H\{^{11}B\})$ 2.40 (s, 1H; B4H), 2.23 (s, 2H; B3H, B5H), 2.20 (s, 1H; C2H), 1.18 (septet, 1H, $J_{HCBH} \sim 4$; (from 100 MHz spectrum); C1H), −2.02 (s, 2H; Hμ).

2,3-$C_2B_4H_8$[25] (2a). (0.3); $\delta(^{11}B)$[26] −0.2 (d, 1B, J_{BHt} = 178; B5), −1.5 (dd, 2B, J_{BHt} = 178, $J_{BH\mu}$ = 46; B4,6), −52.8 (d, 1B, J_{BHt} = 178; B1); $\delta(^1H\{^{11}B\})$[27] 6.47 (s, 2H; CH), 3.60 (s, 1H; B5H), 3.52 (s, 2H; B4H, B6H), −1.03 (s, 1H; B1H), −2.11 (s, 2H; Hμ).

2,4-Me_2-2,3-$C_2B_4H_6$ (2b). (2); $\delta(^{11}B)$ 7.7 (d, 1B, $J_{BH\mu}$ = 44; B4), −1.7 (d, 1B, J_{BHt} = 150; B5), −4.6 (dd, 1B, J_{BHt} = 154, $J_{BH\mu}$ = 48; B6), −48.8 (d, 1B, J_{BHt} = 177; B1); $\delta(^1H\{^{11}B\})$ 5.79 (s, 1H, C3H), 3.44 (s, 1H; B5H), 3.14 (s, 1H; B6H), 2.16 (s, 3H; C2CH_3), 0.59 (s, 3H; B4CH_3), −0.90 (s, 1H; B1H), −1.63 (s, 1H; Hμ(4,5)), −1.99 (s, 1H; Hμ(5,6)).

5-Et-2,3-$C_2B_4H_7$ (2c). (2); $\delta(^{11}B)$ 15.1 (s, 1B; B5), −2.6 (dd, 2B, J_{BHt} = 155, $J_{BH\mu}$ = 52; B4,6), −52.7 (d, 1B, J_{BHt} = 180; B1); $\delta(^1H\{^{11}B\})$ 6.32 (s, 2H; C2,3H), 3.39 (s, 2H; B4,6H), 1.21 (s, 3H; CH_3), 1.14 (s, 2H; CH_2), −0.96 (s, 1H, B1H), −1.56 (s, 2H; Hμ).

2,5-Me_2-2,3-$C_2B_4H_6$ (2d). (0.6); $\delta(^{11}B)$ 13.0 (s, 1B; B5), −3.3 (dd, J_{BHt} = 146, $J_{BH\mu}$ = 49; B4, B6), −48.8 (d, J_{BHt} = 177; B1); $\delta(^1H\{^{11}B\})$ 5.94 (s, 1H; C3H), 3.25 (s, 2H; B4,6H), 2.16 (s, 3H; C2CH_3), 0.60 (s, 3H; B5CH_3), −0.90 (s, 1H; B1H), −1.57 (s, 2H; Hμ).

4-Et-2,3-$C_2B_4H_7$ (2e). (0.2); $\delta(^{11}B)$ 11.1 (d, $J_{BH\mu}$ = 36; B4), −2.0 (d, $J_{BHt} \sim 155$; B5), −4.5 (dd, $J_{BHt} \sim 152$, $J_{BH\mu} \sim 49$; B6), −52.7 (d, $J_{BHt} \sim 180$; B1); $\delta(^1H\{^{11}B\})$ 6.32 (s; C2H), 6.12 (s; C3H), 3.71 (s; B5H), 3.35 (s; B6H), 1.20 (m; CH_2CH_3), −0.96 (s; B1H), −1.60 (s; Hμ(4,5)), −1.94 (s; Hμ(5,6)).

2-Me-2,3,4-$C_3B_3H_6$[1−3,6] (3a). (1.5); $\delta(^{11}B)$ −0.1 (dd, 2B, J_{BHt} = 154, $J_{BH\mu}$ = 53; B5,6), −52.6 (d, 1B, J_{BHt} = 192; B1); $\delta(^1H\{^{11}B\})$ 6.74 (s, 1H; C3H), 5.10 (s, 1H; C4H), 3.37 (s, 2H; B5,6H), 2.13 (s, 3H; CH_3), −0.85 (s, 1H; B1H), −3.66 (s, 1H; Hμ).

1-Me-2,3,4-$C_3B_3H_6$ (3d). (2); $\delta(^{11}B)$ 0.6 (dd, 2B, J_{BHt} = 152, $J_{BH\mu}$ = 66; B5,6), −45.5 (s, 1B; B1); $\delta(^1H\{^{11}B\})$ 7.14 (s, 1H; C3H), 5.38 (s, 2H; C2,4H), 3.53 (s, 2H; B5,6H), −0.45 (s, 3H; B1CH_3), −3.50 (s, 1H; Hμ).

Partial ^{11}B NMR data of the trace products, *i.e.* a 1:5:15 ratio mixture of 2-, 3-, and 4-Me-2-CB_5H_8[28] (**4b**, **4c**, and **4a**) and 2,3,4,5-$C_4B_2H_6$[29] (**5**), were in good agreement with the reported ^{11}B chemical shifts of these known carboranes.[28,30]

Completed Reaction of B_4H_{10} and Ethyne at 70 °C. B_4H_{10} (3 mmol) and ethyne (30 mmol) were held in a sealed 1-liter Pyrex flask at 50 °C for 3 days. The products were then subjected to cold-column fractionation to give several fractions characterized by different mass cutoffs. The separated fractions were identified by boron and proton NMR spectroscopy as **2a** (approximate yield: 5% of total volatile carborane fraction), **2b** (33%), **2c** (27%), **2d** (9%), **2e** (4%), **3a** (21%), **4a**−**c** (0.5%), and **5** (0.2%).

Electron-Diffraction Measurements. Electron-scattering intensities were recorded on Kodak Electron Image plates using the Edinburgh gas-diffraction apparatus operating at *ca.* 44.5 kV (electron wavelength *ca.* 5.7 pm).[31] The scarcity of compound made it unlikely that plates at both long (*s* range 20−144 nm^{-1}) and short (*s* range 60−356 nm^{-1}) camera distances could be recorded successfully. Therefore, as the best alternative, data were recorded at the medium camera distance (nozzle-to-plate distance = 200.89 mm) yielding data in the *s* range 40−224 nm^{-1}. Two plates were obtained with the sample and nozzle held at *ca.* 250 and 291 K, respectively, during the exposure periods.

The scattering pattern of benzene was also recorded for the purpose of calibration; this was analyzed in exactly the same way as those of the carborane to minimize systematic errors in the wavelengths and camera distances. Weighting functions used to set up the off-diagonal weight matrix were $\Delta s = 4$, $s_{min} = 40$, $sw1 = 60$, $sw2 = 192$, and $s_{max} = 224$ nm^{-1}; other experimental parameters were the correlation parameter (−0.3785), final scale factor (0.670(9)), and electron wavelength (5.681 pm).

The electron-scattering patterns were converted into digital form using a computer-controlled Joyce-Loebl MDM6 microdensitometer with a scanning program described previously.[32] The programs used for data reduction[32] and least-squares refinement[33] have been described elsewhere; the complex scattering factors employed were those listed by Ross *et al*.[34]

Microwave Spectroscopy. The spectra (dating from 1970) were measured between 8 and 40 GHz with a 100 kHz Stark-modulated microwave spectrometer. Frequency measurements were made by using interpolation receiver methods with harmonics generated from the crystal-controlled frequency standard of a Hewlett-Packard 5245L frequency counter. The crystal was accurate to 3×10^9. All measurements were made with the sample held at approximately dry ice temperature. Some of the measurements were made on a Hewlett-Packard 8400B−II spectrometer

For measurement of the microwave spectra, a sample of 1,2-$C_2B_3H_7$ was kindly provided by Grimes and co-workers.[5,7] These investigators prepared the sample by a quenched reaction of tetraborane(10) and ethyne in a 10:1 ratio at 70 °C. During the course of the MW studies, the purity of the sample was regularly checked by infrared spectroscopy. The ^{13}C enriched sample was prepared by A. B. Burg from 60% enriched acetylene by passing the precursors through a heated tube and controlling the residence time.[35] The unreacted tetraborane and

(25) Onak, T. P.; Williams, R. E.; Weiss, H. G. *J. Am. Chem. Soc*. **1962**, *84*, 2830.
(26) Onak, T. P.; Drake, R. P.; Dunks, G. B. *Inorg. Chem*. **1964**, *3*, 1686.
(27) Onak, T. P. *Inorg. Chem*. **1968**, *7*, 1043.
(28) Onak, T. P.; Dunks, G. B.; Spielman, J. R.; Gerhart, F. J.; Williams, R. E. *J. Am. Chem. Soc*. **1966**, *88*, 2061.
(29) Onak, T. P.; Wong, G. T. F. *J. Am. Chem. Soc*. **1970**, *92*, 5226.
(30) Onak, T. P.; Tseng, J.; Tran, D.; Correa, M.; Herrera, S.; Arias, J. *Inorg. Chem*. **1992**, *31*, 2161.
(31) Huntley, C. M.; Laurenson, G. S.; Rankin, D. W. H. *J. Chem. Soc., Dalton Trans*. **1980**, 954.
(32) Cradock, S.; Koprowski J.; Rankin, D. W. H. *J. Mol. Struct*. **1981**, *77*, 113.
(33) Boyd, A. S. F.; Laurenson G. S.; Rankin, D. W. H. *J. Mol. Struct*. **1981**, *71*, 217.
(34) Ross, A. W.; Fink, M.; Hilderbrandt, R. *International Tables for Crystallography*; Wilson, A. J. C., Ed.; Kluwer Academic Publishers: Dordrecht, The Netherlands, 1992; Vol. C, p 245.
(35) A. B. Burg, private communication.

acetylene were recycled through the heated tube. The microwave measurements indicated that the doubly substituted ^{13}C isotopic species was prevalent. This indicates that the carbon atoms of the acetylene remain bonded during the course of the synthesis.

Theoretical Calculations. The MP2(full)/6-31G* geometry of 1,2-$C_2B_3H_7$ has been taken from ref 10. Reoptimizations have been performed employing standard methods[36] at the MP2(fc)/TZP level, *i.e.* employing the frozen-core approximation and the following polarized triple-ζ basis set: B, C, Dunning's [5s3p] basis;[37] H, Dunning's [3s] basis,[37] augmented with one set of d-polarization functions on B and C (exponents 0.386 and 0.75, respectively) and with one set of p-polarization functions on hydrogen (exponent 0.75). In addition, higher-level optimizations have been performed at the MP3-(fc)/TZP level (*i.e.* including electron correlation up to third-order Møller−Plesset perturbation theory) and at the CCSD(T)/TZP level (*i.e.* including higher orders of electron correlation, to coupled cluster with single, double, and perturbatively included connected triple excitations).[38] Energies are denoted "level of calculation//level of geometry optimization". The computations employed the Gaussian 94 program package.[39]

Chemical shifts have been computed using the IGLO (individual gauge for localized orbitals)−SCF[40] and the GIAO (gauge-including atomic orbitals)−SCF[41] and −MP2 methods,[42] employing the "direct IGLO"[43] and the Aces II[44] programs, respectively, and the following basis sets: basis II, *i.e.* a Huzinaga[45] basis set contracted to [5s4p] and augmented with one set of d-polarization functions for B and C (exponents 0.7 and 1.0, respectively) and a [3s] basis augmented with one set of p-polarization functions for H (exponent 0.65).[40c] Basis TZP′: TZP for B and C but employing DZP basis for H, *i.e.* Dunning's[46] [2s] basis augmented with one set of p-polarization functions. Theoretical ^{11}B chemical shifts have been referenced to B_2H_6 and converted to the usual $BF_3{\cdot}OEt_2$ scale as described elsewhere.[10]

Results

B_4H_{10}/Ethyne Reaction: Product Analysis. In agreement with earlier reports,[5−7] the major volatile product from the quenched reaction was found to be the unstable dicarbaborane 1,2-$C_2B_3H_7$ (**1**). This comprised 90% of the total volatile fraction under the conditions employed and was produced in an approximate yield of 25%, based on the amount of boron consumed. From the semiquantitative reaction profile in Figure 2, it is apparent that **1** reaches maximum concentration after *ca*. 20 min, just as the ethyne concentration falls to zero. At this stage B_5H_{11}, the main product of the decomposition of B_4H_{10}, begins to accumulate. The best yields of the volatile carboranes were obtained by quenching a 1:2 mixture of B_4H_{10} and HC≡CH which had been heated at 70 °C for *ca*. 45 min. Attempts to decrease the reaction time by increasing the temperature resulted in flash reactions.[47]

The previously unreported boron-decoupled proton spectrum of **1** showed an apparent septet at 1.18 ppm with a coupling constant of ∼4 Hz. This is assigned to the apical proton which couples with all basal protons to give the septet. The behavior is reminiscent of that reported for structurally similar B_5H_9, in which the apical proton gives a nonet in the boron-decoupled proton spectrum from coupling to the eight basal protons.[48]

The minor carboranes, identified by low-resolution mass spectrometry and high-field ^{11}B and ^1H NMR spectroscopy, were 2,3-$C_2B_4H_8$ (**2a**), 2,4-Me_2-2,3-$C_2B_4H_6$ (**2b**), 2,5-Me_2-2,3-$C_2B_4H_6$ (**2d**), 4-Et-2,3-$C_2B_4H_7$ (**2e**), 5-Et-2,3-$C_2B_4H_7$ (**2c**), 2-Me-2,3,4-$C_3B_3H_6$ (**3a**), and 1-Me-2,3,4-$C_3B_3H_6$ (**3d**). When a mixture of B_4H_{10} and excess HC≡CH was left at 50 °C for 3 days, the carborane products were the same as those found from the quenched reactions except that 1,2-$C_2B_3H_7$ (**1**) and 1-$MeC_3B_3H_6$ (**3d**) were absent. It was presumed that these carboranes must have either decomposed, polymerized or reacted further with other species present. The involatile solids from these reactions were not investigated.

Analysis of the Rotational Spectra of 1,2-$C_2B_3H_7$ Isotopomers. Since ^{11}B and ^{10}B isotopes occur in natural abundance in the ratio of 4:1, and since the molecule has a plane of symmetry, the normal and the two species singly substituted at B(3) and B(4) occur in the ratio 0.51:0.26:0.13, respectively. Microwave transitions from some less abundant isotopomers were also observed but have not been assigned.

The rotational spectrum was quite dense with a constant background of weak lines attributed to Q-branches of a myriad of weakly populated isotopic species. However, the R-branch lines were strong and stood out among the background. The rotational constants were first estimated by assuming some "reasonable" bond distances and angles. However, the estimated spectrum was quite different from what was actually observed. After the assignment, it was seen that the asymmetry of the molecule was very sensitive to small differences in the structure of the tetragonal base. A beautiful, easily identified Q-branch was first observed with a bandhead at 28 282 MHz with line spacing of about 1 MHz, indicating that the molecule was that of a very slightly asymmetric oblate rotor. Then the *c*-type $J = 1-0$ transitions for the three isotopic species were identified by their characteristic simple Stark effects. When a second Q-branch was observed, the difference between the A and B rotational constants was determined to be ∼30 MHz. Then the $J = 2-1$ *c*-type transitions were easily identified and confirmed by their Stark effects. Ultimately, *c*- and either *a*- or *b*-type transitions were found for each isotopic species. The observed R-branch transitions used to determine the rotational constants are given in Table 1. It should be noted that the *b*- and *c*-axes interchange with isotopic substitution at B(3) since the base is accidentally symmetric. The Q-branch series, all associated with high *K* values, were not used in the fits and are not reported.

For the ^{13}C isotopic species, only the *c*-type transitions could be assigned confidently. The assigned lines are also given in Table 1. Thus, the C constants have not been well determined as indicated in Table 1 by their values in parentheses.

(36) Hehre, W.; Radom, L.; Schleyer P. v. R.; Pople, J. A. *Ab Initio Molecular Orbital Theory*; Wiley: New York, 1986.
(37) Dunning, T. H. *J. Chem. Phys.* **1970**, *53*, 2823.
(38) (a) Purvis, G. D.; Bartlett, R. J. *J. Chem. Phys.* **1982**, *76*, 1910. (b) Scuseria, G. E.; Janssen, C. L.; Schaefer, H. F., III. *J. Chem. Phys.* **1988**, *89*, 7382. (c) Scuseria, G. E.; Schaefer, H. F., III. *J. Chem. Phys.* **1989**, *90*, 3700.
(39) Frisch, M. J.; Trucks, G. W.; Schlegel, H. B.; Gill, P. M. W.; Johnson, B. G.; Robb, M. A.; Cheeseman, J. R.; Keith, T.; Petersson, G. A.; Montgomery, J. A.; Raghavachari, K.; Al-Laham, M. A.; Zakrzewski, V. G.; Ortiz, J. V.; Foresman, J. B.; Peng, C. Y.; Ayala, P. Y.; Chen, W.; Wong, M. W.; Andres, J. L.; Replogle, E. S.; Gomperts, R.; Martin, R. L.; Fox, D. J.; Binkley, J. S.; Defrees, D. J.; Baker, J.; Stewart, J. P.; Head-Gordon, M.; Gonzalez, C.; Pople, J. A. *Gaussian 94*, Revision B.3; Gaussian, Inc.: Pittsburgh, PA, 1995.
(40) (a) Kutzelnigg, W. *Isr. J. Chem.* **1980**, *19*, 193. (b) Schindler M.; Kutzelnigg, W. *J. Chem. Phys.* **1982**, *76*, 1919. For a review, see: (c) Kutzelnigg, W.; Schindler M.; Fleischer, U. In *NMR Basic Principles and Progress*; Springer-Verlag: Berlin, 1990; Vol. 23, p 165 ff.
(41) (a) Ditchfield, R. *Mol. Phys.* **1974**, *27*, 789. (b) Wolinski, K.; Hinton, J. F.; Pulay, P. *J. Am. Chem. Soc.* **1990**, *112*, 8251.
(42) (a) Gauss, J. *Chem. Phys. Lett.* **1992**, *191*, 614. (b) Gauss, J. *J. Chem. Phys.* **1993**, *99*, 3629.
(43) Meier, U.; Wüllen, C. v.; Schindler, M. *J. Comput. Chem.* **1992**, *13*, 551.
(44) Stanton, J. F.; Gauss, J.; Watts, J. D.; Lauderdale, W. J.; Bartlett, R. J. *Int. J. Quantum Chem. Symp.* **1992**, *26*, 879.
(45) Huzinaga, S. *Approximate Atomic Wave Functions*; University of Alberta: Edmonton, Alberta, 1971.
(46) Dunning, T. H. *J. Chem. Phys.* **1970**, *53*, 2823.
(47) Grimes, R. N.; Bramlett, C. L.; Vance, R. L. *Inorg. Chem.* **1968**, *8*, 55.
(48) Onak, T. P. *J. Chem. Soc., Chem. Commun.* **1972**, 351.

Table 1. Assigned Microwave Transitions and Constants of 1,2-$C_2B_3H_7$ for all Studied Isotopomers[a]

	isotopomer						
transition/constant	normal	^{10}B(3)	^{10}B(4)	^{13}C(1)	^{13}C(2)	^{13}C(1,2)	^{13}C(1,2)^{10}B(3)
c-type							
$1_{10} - 0_{00}$	16317.83	16531.82	16547.60	16136.76	16146.42	15967.90	16176.60
$2_{21} - 1_{11}$	32663.76	32833.98	33284.80	32303.20	32478.72	32118.88	32710.82
$2_{11} - 1_{01}$	32606.87	33293.48	32905.91	32243.34		31752.34	31994.60
$2_{20} - 1_{10}$	32635.62	33079.21	33105.45	32273.93	32303.20	31945.71	
a-type							
$3_{03} - 2_{02}$	36097.45						
$3_{13} - 2_{12}$							
b-type							
$3_{03} - 2_{12}$		36661.75	36711.68				
$3_{13} - 2_{02}$		36676.40	36722.43				
A	8173.05	8380.81	8368.569	8083.214	8166.15	8075.537	8272.23
B	8144.61	8151.06	8179.121	8053.329	7980.27	7892.268	7914.12
C	5587.76	5680.998	5688.906	(5586)[b]	(5533)[b]	(5512)[b]	(5602)[b]
I_a	61.8534	60.3201	60.4083	62.54022		62.6003	
I_b	62.0694	62.0203	61.8075	62.77292		64.0540	
I_c	90.4712	88.9863	88.8626	(90.48)[b]		(91.70)[b]	

[a] All frequencies are in MHz with errors ±0.05 MHz, *B*/MHz, *I*/kg m^2. [b] Values in parentheses were not well determined.

Table 2. Structural Parameters for the GED Study of 1,2-$C_2B_3H_7$ (r_α°/pm, $\angle_\alpha$/°)[a,b]

no.	parameter	
1	*r*[B(3)−B(4)]	185.7(3)
2	B(3)−B(4)−B(5)	80.9(1)
3	$^1/_5${2*r*[C(1)−B(3)] + 2*r*[C(2)−B(3)] + *r*[C(1)−B(4)]}	157.8(1)
4	B(3)−B(4)−B(5)/B(3)−B(5)−C(2)	2.7(6)
5	*r*[C(1)−B(3)] − $^1/_3${*r*[C(1)−B(4)] + 2*r*[C(2)−B(3)]}	6.1(5)
6	*r*[C(1)−B(4)] − *r*[C(2)−B(3)]	3.1(5)
7	*r*[B−H$_t$] (mean)	119.2(4)
8	C(1)−B(4)−H(4)	128.0(9)
9	*r*[C−H] (mean)	109.3(5)
10	B(4)−C(1)−H(1)	132.8(7)
11	C(1)−C(2)−H(2)	118.8(6)
12	*r*[B−H$_\mu$] (mean)	135.7(6)
13	*r*[B(3)−H(3,4)] − *r*[B(4)−H(3,4)]	3.0(6)
14	B(3)−B(4)−B(5)/B(3)−H(3,4)−B(4)	61.0(6)
15	H(3) wag	2.4(4)
16	H(3) tilt	10.8(10)

[a] For definitions of the parameters and details of the refinement conditions, see the text. [b] Figures in parentheses are the estimated standard deviations.

Analysis of Electron-Diffraction Data for 1,2-$C_2B_3H_7$. Model. When molecular C_s symmetry was assumed, the atomic coordinates for 1,2-$C_2B_3H_7$ were defined by the 16 independent geometrical parameters listed in Table 2. With reference to the numbering system in Figure 1, the distance parameters were B(3)−B(4), p_1; the mean B−C distance, p_3; the difference between C(1)−B(3) and the mean of the other B−C distances, p_5; the difference between C(1)−B(4) and C(2)−B(3), p_6; the mean of the terminal B−H distances, p_7, with all differences from this mean fixed at the *ab initio* [CCSD(T)/TZP′ level] values, and an analogous definition, p_9, for the C−H distances; a mean, p_{12}, of and a difference, p_{13}, between the bridging B−H distances. The angles included B(3)−B(4)−B(5), p_2, C(1)−B(4)−H(4), p_8, B(4)−C(1)−H(1), p_{10}, and C(1)−C(2)−H(2), p_{11}; the angles between the plane B(3)−B(4)−B(5) and the planes B(3)−B(5)−C(2), p_4, and B(3)−H(3,4)−B(4), p_{14}; the H(3) wag, p_{15}, defined as the acute angle subtended between the B(3)···B(5) vector and the projection of B(3)−H(3) onto the B(3)−B(4)−B(5) plane, measured positive as H(3) moves toward C(2); and the H(3) tilt, p_{16}, defined as the acute angle subtended between B(3)−H(3) and the B(3)−B(4)−B(5) plane, measured positive as H(3) moves toward C(1).

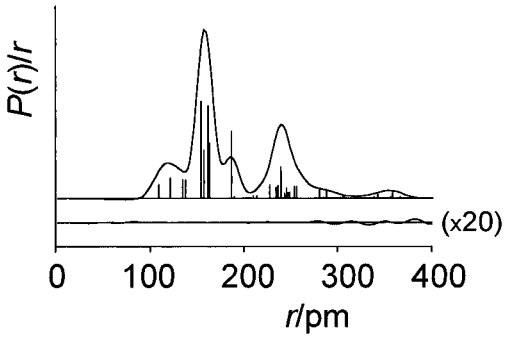

Figure 3. Observed and final weighted difference (×20) radial-distribution curves for 1,2-$C_2B_3H_7$. Before Fourier inversion the data were multiplied by $s \exp[(-0.000\ 02s^2)/(Z_c - f_c)(Z_B - f_B)]$.

Refinement. The radial-distribution curve for 1,2-$C_2B_3H_7$ (Figure 3) shows three peaks in the bonding region at *ca*. 119, 161, and 189 pm. These are assigned to the X−H (X = B, C) distances, the C−C and B−C distances, and the B−B distances, respectively. Above 200 pm, the most intense peak lies at *ca*. 242 pm and is associated with the heavy-atom C(2)···B(4) and B(3)···B(5) nonbonded distances and the two-bond X···H nonbonded pairs. The shoulder at *ca*. 287 pm and the broad peak centered at *ca*. 358 pm arise principally from two-bond B(3)/B(4)···H scattering and from three-bond X···H scattering, respectively.

The r_α° structure of 1,2-$C_2B_3H_7$ was refined. A harmonic vibrational force field was computed at the MP2/6-31G* level, and the Cartesian force constants were transformed into those described by a set of symmetry coordinates using the program ASYM40.[49] As a full analysis of experimental vibrational frequencies is not available for the compound, it was not possible to scale the theoretical force constants on this basis. Instead, as the best alternative, empirical scale factors of 0.9 for bond stretches, 0.85 for bends, and 0.8 for out-of-plane bends, and torsions were employed.[50] Values for the root-mean-square amplitudes of vibration (*u*), perpendicular amplitude corrections (*K*), and harmonic vibrational corrections ($B_0 \rightarrow B_z$) were then derived from the scaled force constants using ASYM40.[49]

(49) *ASYM40*, version 3.0, update of program ASYM20, in: Hedberg, L.; Mills, I. M. *J. Mol. Spectrosc.* **1993**, *160*, 117.
(50) For example, see: Rauhut, G.; Pulay, P. *J. Phys. Chem.* **1995**, *99*, 3093 and references therein.

Table 3. Interatomic Distances (r_a/pm) and Amplitudes of Vibration (u/pm) for the GED Study of 1,2-$C_2B_3H_7$[a,b]

no.	interatomic pair	distance	u(expt)[c]	u(calc)[c]
1	C(2)−B(3)	154.4(2)	5.1(1)	5.4
2	C(1)−B(4)	157.5(5)	5.2 }	5.6
3	C(1)−B(3)	161.5(3)	5.6 } (tied to u_1)	6.0
4	C(1)−C(2)	162.6(6)	5.7 }	6.0
5	B(3)−B(4)	185.8(3)	6.4(2)	6.7
6	C(1)−H(1)	110.5(5)[d]	7.7(5)	7.6
7	C(2)−H(2)	111.0(5)[d]	7.8 (tied to u_6)	7.7
8	B(3)−H(3)	120.6(4)[d]	9.1(7)	8.3
9	B(4)−H(4)	120.5(4)[d]	9.1 (tied to u_8)	8.3
10	B(4)−H(3,4)	134.6(7)	10.3(6)	10.5
11	B(3)−H(3,4)	137.6(6)	10.7 (tied to u_{10})	10.9
12	C(1)/C(2)···H (two bond)	228.2−256.3	10.8−12.7(6)	10.4−12.2
13	B(3)/B(4)···H (two bond)	236.2−254.6	8.2−9.5(7)	10.6−12.3
14	B(3)/B(4)···H (two bond)	280.1−286.4	11.3−11.5(7)	11.8−12.0
15	C(2)···B(4)	237.7(1)	5.5(2)	6.0
16	B(3)···B(5)	240.9(2)	5.5 (tied to u_{15})	6.0
17	B,C···H (three bond)	343.1−359.0	9.6−10.0(7)	9.5−9.9

[a] For atom numbering scheme, see Figure 1. Figures in parentheses are the estimated standard deviations. [b] H···H nonbonded distances were also included in the refinements but are not lited here. [c] Key: expt = GED refinement; calc = calculated from the scaled theoretical force field. [d] For the X−H (X = B, C) distances, the difference from the mean value was fixed at the theoretical (CCSD(T)/TZP′) value in the $r_\alpha°$ refinement.

The refinement procedure combined a simultaneous fitting of both the electron-diffraction data and the vibrationally corrected rotation constants for 1,2-$C_2B_3H_7$. However, although B_z values are available for seven isotopomers, those for the species involving ^{13}C were considered to be less reliable since only the *c*-type transitions had been assigned. Subsequently, only B_z values for the normal and ^{10}B singly substituted species were used in the structure refinements.

Using starting values taken from the structure optimized *ab initio* at the MP2/TZP level (the highest level available to us at the time), it was possible to refine simultaneously all of the parameters pertaining to the C_2B_3 cage geometry, p_{1-6}, together with those defining the mean X−H (X = B, C) distances, p_7, p_9, and p_{12}. Attempts to introduce the other parameters defining the hydrogen-atom positions, p_8, p_{10}, p_{11}, and p_{13-16}, either caused the refinement to become unstable (large oscillations in the R_G factor between cycles) or led such parameters to adopt unrealistic values. Attempts were made subsequently to refine these parameters by the SARACEN method, using flexible restraints.[51]

Flexible restraints may allow the refinement of parameters which would otherwise have to be fixed. Estimates of the values of these restrained quantities and their uncertainties are used as additional observations in a combined analysis similar to those routinely carried out for electron-diffraction data combined with rotation constants and/or dipolar coupling constants.[52] The values and uncertainties for the extra observations are derived from another method such as X-ray diffraction or theoretical computations. *All* geometrical parameters are then included in the refinements. In cases where a restraint corresponds exactly to a refined parameter, if the intensity pattern contains useful information concerning the parameter, it will refine with an esd less than the uncertainty in the corresponding additional observation. However, if there is essentially no relevant information, the parameter will refine with an esd equal to the uncertainty of the extra observation and its refined value will equal that of the restraint. In this case, the parameter can simply be fixed, in the knowledge that doing this does not influence either the magnitudes or the esd's of other parameters. In some cases, because increasing the number of refining parameters allows all effects of correlation to be considered, some esd's may increase. Overall, this approach utilizes all available data as fully as possible and returns more realistic esd's for refining parameters; the unknown effects of correlation with otherwise fixed parameters are revealed and included.

Values of flexible restraints applied to independent parameters were derived from the CCSD(T)/TZP′ level optimization and their uncertainties from the variations across the series of *ab initio* computations at correlated levels of theory, as detailed elsewhere.[51a] These restraints were $p_8 = 127.2 \pm 1.2°$, $p_{10} = 132.8 \pm 0.8°$, $p_{11} = 118.4 \pm 0.6°$, $p_{13} = 3.0 \pm 0.6$ pm, $p_{14} = 61.4 \pm 0.7°$, $p_{15} = 2.3 \pm 0.4°$, and $p_{16} = 10.5 \pm 1.1°$.

In addition, ten amplitudes of vibration were included in the final refinements, all subject to restraints derived from the scaled MP2/6-31G* force field with uncertainties of 10% of their absolute starting values. For those amplitudes refining together in groups, the ratios within each group were fixed at the force-field values. The restraints were $u_1 = 5.4 \pm 0.5$ pm, $u_5 = 6.7 \pm 0.7$ pm, $u_6 = 7.6 \pm 0.8$ pm, $u_8 = 8.3 \pm 0.8$ pm, $u_{10} = 10.5 \pm 1.1$ pm, $u_{12} = 10.4 \pm 1.0$ pm, $u_{13} = 10.8 \pm 1.1$ pm, $u_{14} = 12.0 \pm 1.2$ pm, $u_{15} = 6.0 \pm 0.6$ pm, and $u_{17} = 9.9 \pm 1.0$ pm.

Values of the principal interatomic distances for the final refinement ($R_G = 0.014$, $R_D = 0.021$) are listed in Table 3, and the fit to the corrected experimental rotation constants is shown in Table 4. The most significant values of the least-squares correlation matrix are given in Table 5. The experimental and difference radial-distribution curves are shown in Figure 3, and the molecular-scattering intensities are shown in Figure 4. Cartesian coordinates, including those for the CCSD/TZP′ level optimization, are listed in Table 6 together with absolute energies of the theoretical and experimental structures.

Discussion

Mechanistic Considerations. Franz and Grimes have suggested that the initial product, 1,2-$C_2B_3H_7$ (**1**), is probably formed *via* {B_4H_8} (Scheme 1),[6] whereas McKee has computed routes involving both {B_3H_7}[14] and {B_4H_8}[15] and a common intermediate[53] (Scheme 2). Interestingly, the activation barrier for elimination of H_2 from B_4H_{10} is calculated to be somewhat

(51) (a) Blake, A. J.; Brain, P. T.; McNab, H.; Miller, J.; Morrison, C. A.; Parsons, S.; Rankin, D. W. H.; Robertson, H. E.; Smart, B. A. *J. Phys. Chem.* **1996**, *100*, 12280. (b) Brain, P. T.; Morrison, C. A.; Parsons, S.; Rankin, D. W. H. *J. Chem. Soc., Dalton Trans.* **1996**, 4589.

(52) For example, see: Abdo, B. T.; Alberts, I. L.; Attfield, C. J.; Banks, R. E.; Blake, A. J.; Brain, P. T.; Cox, P. T.; Pulham, C. R.; Rankin, D. W. H.; Robertson, H. E.; Murtagh, V.; Heppeler, A.; Morrison, C. A. *J. Am. Chem. Soc.* **1996**, *118*, 209.

Table 4. Microwave Rotation Constants (B/MHz) Used in the GED Study of 1,2-$C_2B_3H_7$

constant[a]	observed (B_0)[b]	corrected (B_z)	calculated (B_z)	ΔB_z (obsd − calcd)	uncertainty[c]	weight[d]
normal species						
A	8173.06(5)	8165.93	8166.48	−0.55	0.71	0.005
B	8144.62(5)	8138.79	8138.53	0.26	0.58	0.007
C	5587.70(5)	5584.97	5584.94	0.03	0.27	0.034
^{10}B(3)						
A	8380.81(5)	8373.68	8373.91	−0.23	0.71	0.005
B	8151.06(5)	8145.09	8145.06	0.03	0.60	0.007
C	5681.00(5)	5678.20	5678.37	−0.17	0.29	0.030
^{10}B(4)						
A	8368.57(5)	8361.27	8361.71	−0.44	0.73	0.005
B	8179.12(5)	8173.29	8172.86	0.43	0.58	0.007
C	5688.91(5)	5686.12	5686.05	0.07	0.28	0.032

[a] For atom-numbering scheme, see Figure 1. [b] Figures in parentheses are the estimated standard deviations. [c] Uncertainty = [(uncertainty in microwave measurement)^2 + 0.1(vibrational correction)^2]$^{1/2}$. [d] Relative to the GED data.

Table 5. Correlation Matrix (×100) for the GED Study of 1,2-$C_2B_3H_7$[a]

p_2	p_4	p_5	p_6	p_7	p_8	p_{10}	p_{12}	p_{16}	u_1	u_6	u_8	u_{14}	u_{16}	k	
−84		63		−59						70				89	p_1
		−52					54			−59				−82	p_2
	−73						60								p_3
						55		−79							p_4
														57	p_5
									59						p_6
										−50					p_7
						−55									p_8
											81		−56		p_9
											−75			−59	p_{12}
														62	u_6
													−50		u_8
												54		61	u_{12}

[a] Only absolute values ≥50 are shown. k is the scale constant.

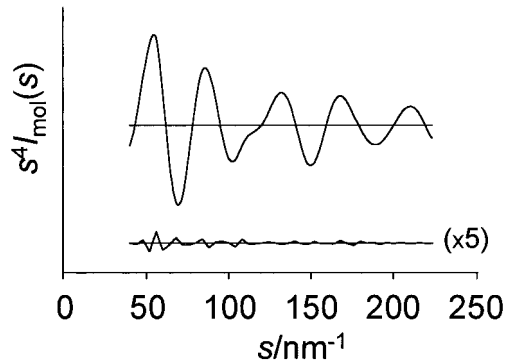

Figure 4. Observed and final weighted difference (×5) molecular-scattering intensity curves for 1,2-$C_2B_3H_7$. The nozzle-to-plate distance was 201 mm.

less than that for elimination of $\{BH_3\}$, which might be thought to favor the former route. There are also two key pieces of kinetic evidence which have been interpreted as favoring the involvement of $\{B_4H_8\}$ as the prime reactive intermediate in thermolysis reactions of B_4H_{10}. First, in the very early stages of the decomposition of B_4H_{10} itself, the initial rate of production of dihydrogen matches very closely the rate of consumption of B_4H_{10},[54] and the same is true in the B_4H_{10}/HC≡CH reaction.[6] Secondly, B_2H_6 is not produced at any significant rate in the initial stages of the thermolysis of B_4H_{10} at 40 °C;[54] it does appear eventually but is probably formed by decomposition of the B_5H_{11} produced in the reaction. In contrast, B_5H_{11}[55] and B_6H_{12},[21] both of which are thought to decompose mainly *via* elimination of $\{BH_3\}$, each generate B_2H_6 from the outset in their thermolysis reactions, at the rate of 0.5 mol per mole of borane. This is consistent with rapid recombination of the $\{BH_3\}$ moieties released in these two decompositions.

Thus the body of experimental evidence is best interpreted in terms of a rate-determining elimination of H_2 from B_4H_{10}, to give $\{B_4H_8\}$. This intermediate can then react with ethyne to give $\{C_2B_4H_{10}\}$, which in turn releases $\{BH_3\}$ to give **1**, as first suggested by Franz and Grimes. The $\{C_2B_4H_{10}\}$ could also lose H_2 to form 2,3-$C_2B_4H_8$ (**2a**), which we observe in this reaction for the first time (Scheme 3).

Regarding the minor products, Franz and Grimes have explained the formation of the tricarbahexaborane **3a** in terms of the addition of two molecules of ethyne to $\{B_4H_8\}$ to give the reactive intermediate $\{C_4B_4H_{12}\}$, followed by loss of $\{BH_3\}$ from the latter (Scheme 1). McKee, on the other hand, has computed a route involving $\{B_3H_7\}$ (Scheme 2). In this regard, it may be significant that the dicarbahexaboranes identified for the first time in this study, **2b**−**e**, all have the molecular formula $C_4B_4H_{12}$, and could therefore be formed by rearrangement of the same intermediate (Scheme 3). The new tricarbahexaborane **3d**, like its isomer **3a**, could also be formed from this complex intermediate by elimination of $\{BH_3\}$ as indicated. We therefore prefer the simplified mechanism shown in Scheme 3, which emphasizes the role of $\{B_4H_8\}$. The unusual $\{CBH_3\}$-abstraction proposed by Franz and Grimes is no longer necessary and is omitted from Scheme 3.

Acetylenic C−C bond cleavage is evident in the formation of the products **2b**, **2d**, and **3d**, and acetylenic C−H cleavage has taken place in the formation of **2b**, **2d**, and **3a**. The

(53) This intermediate is the open cyclic form of 1,2-$C_2B_3H_7$ numbered **15** in ref 14 and **6** in ref 15.

(54) Greatrex, R.; Greenwood, N. N.; Potter, C. D. *J. Chem. Soc., Dalton Trans.* **1986**, 81.

(55) Attwood, M. D.; Greatrex, R.; Greenwood, N. N. *J. Chem. Soc., Dalton Trans.* **1989**, 385; 391.

Table 6. Cartesian Coordinates (pm) for 1,2-$C_2B_3H_7$

atom	*x*	*y*	*z*	*x*	*y*	*z*
	(a) Combined GED/MW Refinement			(b) Theoretical (CCSD/TZP′ Level) Optimization		
C(1)	0.00	23.90	104.78	0.00	25.68	106.11
C(2)	0.00	−96.38	−4.58	0.00	−96.25	−3.02
B(3)	−120.44	0.00	0.00	−121.00	0.00	0.00
B(4)	0.00	141.32	0.00	0.00	142.44	0.00
B(5)	120.44	0.00	0.00	121.00	0.00	0.00
H(1)	0.00	21.94	213.70	0.00	24.65	214.11
H(2)	0.00	−200.16	31.06	0.00	−198.59	33.81
H(3)	−237.49	−4.91	22.28	−237.50	−4.60	21.57
H(4)	0.00	258.58	21.12	0.00	258.92	21.66
H(5)	237.49	−4.91	22.28	237.50	−4.60	21.57
H(3,4)	−95.32	103.48	−86.49	−94.88	103.22	−85.98
H(4,5)	95.32	103.48	−86.49	94.88	103.22	−85.98

(c) Absolute Energies (Hartrees) of the Theoretical and Experimental Structures

	geometry				
level	MP2/6-31G*	MP2/TZP	MP3/TZP	CCSD(T)/TZP′	GED
SCF/II	153.82830		153.82889	153.82820	153.82777
SCF/TZP	153.83419	153.83475	153.83505	153.83447	153.83393
MP2/6-31G*	154.34820				
MP2/TZP	154.42459	154.42512	154.42506	154.42494	154.42458
MP3/TZP	154.46155	154.46225	154.46232	154.46216	154.46167
MP4sdtq/TZP	154.49520	154.49618	154.49622	154.49634	154.49581
CCSD(T)/TZP	154.49465	154.49561	154.49566	154.49577	154.49527

Scheme 3

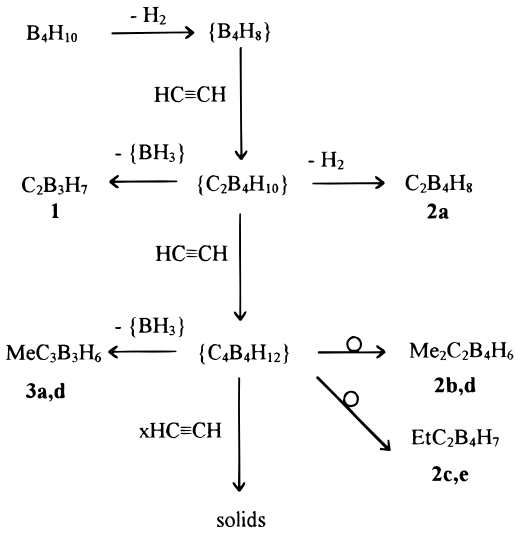

structures of the complex carbatetraborane intermediates involved in the formation of these various products are not known; *arachno*-2,5-μ-CH_2-1-CB_4H_8 (**6**), alkyl derivatives of which have been isolated recently from quenched reactions of B_4H_{10} with propyne and butynes,[16] may not be the only candidate for $\{C_2B_4H_{10}\}$, and the suggestion by a referee that $\{C_4B_4H_{12}\}$ could be the hydroboration product $\{(H_2C{=}CH)C_2B_4H_9\}$ remains speculative. Nevertheless, the proposal that the latter could then rearrange by internal hydroboration (as found for the vinylpentaboranes[56]), accompanied by BH_3 loss and insertion of the α-vinyl carbon, eventually to give the tricarbaboranes **3a**, and **3d**, has considerable appeal.

Also of mechanistic interest, but difficult to rationalize, is the fact that the products containing B-alkyl groups show clear preferences for substitution at a particular position. Thus, the isomers **2b** and **2d** in the dimethyl system B,2-$Me_2C_2B_4H_6$ constitute respectively 33 and 9% of the volatile fraction in the completed reaction, indicating that the basal B4 atom adjacent to carbon is the favored position for substitution. In contrast, in the B-$EtC_2B_4H_7$ system, in which **2c** makes up 27% and **2e** 4% of the fraction, the B5 position remote from carbon is clearly favored, and in the B-$MeC_3B_3H_6$ system, boron substitution occurs at the apical B1 site only, to give **3d**. Some preference for substitution at the B4 position remote from carbon, compared with the B3 site adjacent to carbon, was indicated for the monocarbapentaboranes 4- and 3-$MeCB_5H_8$, **4a** and **4c**. Trace amounts of these were identified by ^{11}B NMR spectroscopy, together with the carbon-substituted isomer **4b**; the three isomers, **4a**, **4c**, and **4b**, were present in the ratio 15:5:1.

The tetracarbahexaborane **5** was also identified in trace amounts, and is likely to be formed by reaction of **1** with ethyne.[8] Reactions of B_5H_9 and ethyne at 215−225 °C[27,29] and flash thermolysis of 2-$H_2C{=}CHB_5H_8$ at 355 °C[56] were shown to give mixtures of isomers of Me-2-CB_5H_8 in which acetylenic C−H or C−C cleavage had clearly taken place. The observation of these derivatives at the lower temperature (70 °C) used in the present study suggests the availability of a low-energy route for their formation.

No new carboranes with novel structures, such as those of the type computed by McKee,[14,15] have been observed in the present work. Therefore, in contrast to the wide range of known *nido*-carbahexaboranes, *e.g.* 2-CB_5H_9,[29] 2,3-$C_2B_4H_8$,[57] 2,3,4-$C_3B_3H_7$,[18] and 2,3,4,5-$C_4B_2H_6$,[58] only one *nido*-carbapentaborane, 1,2-$C_2B_3H_7$ (**1**), has been reported to date.[5−7,11] We now report the results of a study of the molecular structure of this compound in the gas phase.

Electron-Diffraction Study of 1,2-$C_2B_3H_7$. The gas-phase electron-diffraction pattern of 1,2-$C_2B_3H_7$ is consistent with a geometry having C_s symmetry, similar to that of pentaborane-(9). The apical position is occupied by a carbon atom, displaced toward B(4) from a position directly above the B(5)···B(3) vector, and hydrogen atoms asymmetrically bridge the B−B bonds (Figure 1a). The basal atoms are almost coplanar, C(2) lying *ca*. 2° below the B(3)−B(4)−B(5) plane.

(56) Wilczynski, R.; Sneddon, L. G. *Inorg. Chem.* **1981**, *20*, 3955.

(57) Cendrowski-Guillaume, S. M.; Spencer, J. T. *Organometallics* **1992**, *11*, 969 and references therein.

(58) Herberhold, M.; Bertholdt, U.; Milius, W.; Glöcke, A.; Wrackmeyer, B. *Chem. Commun.* **1996**, 1219 and references therein.

Table 7. Geometrical Parameters (*r*/pm, ∠/°) from the Theoretically Optimized (r_e) Structures of 1,2-$C_2B_3H_7$

	level/basis set					
parameter[a]	SCF/6-31G*	MP2/6-31G*	MP2/TZP	MP3/TZP	CCSD(T)/TZP′	GED (r_α°)[b]
C(1)−C(2)	162.0	160.7	162.4	162.5	163.6	162.6(6)
C(1)−B(3)	161.4	161.1	162.3	162.4	163.0	161.4(3)
C(2)−B(3)	152.5	153.8	154.2	154.1	154.6	154.3(2)
C(1)−B(4)	157.2	156.4	157.2	157.5	157.8	157.4(5)
B(3)−B(4)	187.1	184.0	186.0	186.7	186.9	185.7(3)
C(2)−H(2)	107.5	108.6	108.4	108.2	108.8	109.7(5)[c]
C(1)−H(1)	106.9	108.0	107.6	107.4	108.0	108.9(5)[c]
B(3)−H(3)	117.9	118.6	118.2	118.2	118.6	119.3(4)[c]
B(4)−H(4)	117.9	118.6	118.1	118.1	118.5	119.2(4)[c]
B(3)−H(3,4)	138.3	135.7	136.4	136.8	136.9	137.2(6)
B(4)−H(3,4)	132.3	133.1	133.7	133.6	133.9	134.2(7)
B(3)−B(4)−B(5)	79.8	81.3	80.9	80.6	80.7	80.9(1)
B(4)−C(1)−H(1)	132.2	132.1	132.9	132.7	132.8	132.8(7)
C(1)−B(4)−H(4)	127.0	126.3	127.3	127.5	127.2	128.0(9)
C(1)−C(2)−H(2)	119.0	119.0	118.5	118.6	118.4	118.8(6)
B(3)−B(4)−B(5)/ B(3)−B(4)−H(3,4)	59.3	61.4	62.1	61.4	61.4	61.0(6)
B(3)−B(4)−B(5)/ B(3)−B(5)−C(2)	2.4	1.2	1.6	1.6	1.8	2.7(6)
H(3) wag	2.9	1.9	2.0	2.2	2.3	2.4(4)
H(3) tilt	9.4	11.3	10.5	10.2	10.5	10.8(10)

[a] For atom numbering scheme see Figure 1. For definitions of parameters see the text. [b] Figures in parentheses are the estimated standard deviations. [c] For the X−H (X = B, C) distances, the difference from the mean value was fixed at the theoretical (CCSD(T)/TZP′) value in the r_α° refinement.

Geometrical parameters derived from the theoretically optimized computations, defining the equilibrium (r_e) structure, are given in Table 7. In general, the heavy-atom cage bond distances shorten with the introduction of electron correlation and lengthen on moving to higher correlated levels [C_2B_3 cage distances (mean, in pm): SCF/6-31G*, 165.2; MP2/6-31G*, 164.4; MP2/TZP, 165.6; MP3/TZP, 165.8; CCSD(T)/TZP′, 166.3]. At correlated levels, variations in other bond distances and angles are small, being of the order of 1 pm and 1°, respectively. At the highest level available to us [CCSD(T)/TZP′], the theoretical values are generally in very good agreement with those refined experimentally by GED. At 161.4(3) pm, the distance C(1)−B(3) is refined to a value significantly (99% confidence level) shorter than that predicted *ab initio* at the coupled cluster level (163.0 pm). A basis set larger than TZP′ is likely to shorten bond lengths and improve this agreement, but such computations are beyond our resources. Note also that experimental distances are for a vibrationally averaged (r_α°) structure rather than a theoretical equilibrium (r_e) structure.

The reliability of the final GED structure is supported by the results of theoretical chemical-shift calculations shown in Table 8. Computations have been performed using both the IGLO and GIAO methods for the GED and several of the theoretical structures. The overall fit to the experimental δ values for each geometry (as judged by the root-mean-square difference) improves by *ca.* 2 ppm on changing from the IGLO to the GIAO method at the SCF level. However, the importance of electron correlation in such computations is demonstrated by moving to the GIAO−MP2 method, whereby a further improvement in RMS fit of *ca.* 3−4 ppm is observed. The basis of this marked improvement for all geometries centers around the ^{13}C chemical shifts. Only with the GIAO−MP2 method are these computed to be within a few ppm of the experimental values. In contrast, the ^{11}B shifts are computed to lie within similar error ranges using both the uncorrelated IGLO−SCF and GIAO−SCF methods. The GED and CCSD(T)/TZP′ level geometries perform almost equally well using GIAO−MP2; the maximum absolute deviations from the $\delta(^{11}B)$ and $\delta(^{13}C)$ experimental values are 0.9 and 2.3 ppm (GED) and 0.4 and 3.4 ppm (*ab initio*), respectively.

Table 8. Theoretical Chemical Shifts (δ/ppm[a]) for the Theoretical and Experimental Geometries

method	geometry	B(3,5)	B(4)	C(1)	C(2)	ΔRMS[b]
IGLO−SCF	MP2/6-31G*	−13.9	−15.7	−34.8	48.8	7.2
	MP3/TZP	−12.6	−15.6	−36.2	51.4	7.2
	CCSD(T)/TZP′	−12.4	−15.5	−35.1	53.6	6.4
	GED	−12.6	−15.8	−34.4	52.6	6.3
GIAO−SCF	MP2/6-31G*	−13.3	−14.7	−30.5	51.7	4.9
	MP3/TZP	−12.1	−14.7	−32.3	54.2	5.2
	CCSD(T)/TZP′	−11.8	−14.5	−31.2	56.3	4.5
	GED	−12.1	−14.9	−30.5	55.2	4.3
GIAO−MP2	MP2/6-31G*	−14.6	−16.0	−23.1	57.4	1.1
	MP3/TZP	−13.3	−15.7	−24.4	59.4	1.5
	CCSD(T)/TZP′	−13.0	−15.5	−23.3	61.3	1.7
	GED	−13.3	−16.0	−22.9	60.2	1.3
experiment[c]		−13.4	−15.1	−21.5	57.9	

[a] Relative to BF_3·OEt_2 for ^{11}B and Me_4Si for ^{13}C. [b] Root-mean-square difference between the five experimental and theoretical chemical shifts. [c] This work.

Table 9. Relative Energies (kJ mol^{-1}) of the GED Geometry

level	rel energy[a]
SCF/TZP	1.4
MP2/TZP	0.9
MP3/TZP	1.3
MP4sdtq/TZP	1.4
CCSD(T)/TZP	1.3

[a] Relative to the CCSD(T)/TZP′ geometry.

Single-point energy calculations (Table 9) for the GED geometry have been performed at various levels. At the CCSD(T)/TZP level, the final experimental structure lies just 1.3 kJ mol^{-1} above the fully optimized CCSD(T)/TZP′ structure. Thus, on the basis of the experimental and theoretical criteria (*R* value, computed chemical shifts, and relative evergy), the combined GED/MW geometry (refined using restraints derived from *ab initio* computations) offers an accurate and reliable description of the molecular structure of 1,2-$C_2B_3H_7$.

Previous computations[10−12] concluded that the structure of 1,2-$C_2B_3H_7$ derived from a preliminary analysis of lines in the microwave spectrum[9] is incorrect. This conclusion is now confirmed experimentally by GED. Interestingly, the earlier MW-alone structure contains a C−C bond length of 145.3 pm, *ca*. 9 pm shorter than the sum of the covalent radii, implying that some double-bond character is retained in the cage. Conversely, however, the correct structure indicates that the C−C bond, at 162.6(6) pm, has less than a single-bond order.

It is pleasing to note that the structure now established for 1,2-$C_2B_3H_7$, both experimentally and theoretically, possesses the geometry originally proposed by Franz and Grimes,[5] as based on a comparison of the simulated and experimental ^{11}B and ^{1}H NMR spectra of the compound.

Summary and Conclusions

The quenched gas-phase reacton of B_4H_{10} and ethyne at 70 °C has been shown to give a wider variety of *nido*-carboranes than reported earlier, including derivatives that are formed by acetylenic C−C and/or C−H bond cleavages. The molecular structure of the major volatile product, 1,2-$C_2B_3H_7$ (**1**), the only carbapentaborane reported to date, has been successfully determined by a combined GED/MW refinement restrained by *ab initio* computations. New carborane products identified in this study were alkyl derivatives of 2,3-$C_2B_4H_8$ (**2b**−**e**), two of which had previously been identified incorrectly as tricarbaboranes, and 1-Me-2,3,4-$C_3B_3H_6$ (**3d**). No new types of carborane structure were observed in this particular reaction, and further advances in our understanding of the mechanism involved in this and related systems will, we believe, depend on the outcome of future studies of reactions of B_4H_{10} with other alkynes and on more detailed theoretical investigations.

Acknowledgment. We thank the EPSRC for financial support of the synthetic work at Leeds and the Edinburgh Electron Diffraction Service (Grant GR/K44411), including research fellowships to P.T.B., M.A.F., and H.E.R. and provision of the microdensitometer facilities at the Daresbury Laboratory. A.N. was supported by a studentship from the Ministry of Culture and Higher Education of the Islamic Republic of Iran. M.B. gratefully acknowledges generous support by Prof. W. Thiel. We thank the Royal Society for financial assistance and Dr. L. Hedberg (Oregon State University) for a copy of the program ASYM40. Calculations were performed on IBM RS6000 workstations of the Competence Center for Computational Chemistry at the ETH Zürich and on a NEC SX4 supercomputer of the Centro Svizzero di Calcolo Scientifico at Manno, Switzerland.

IC971395Z